Research Report

Addressing Long-Standing Chemical Challenges by AFM with Functionalized Tips

Diego Peña[1], Niko Pavliček[2,4], Bruno Schuler[2,3], Nikolaj Moll[2], Dolores Pérez[1], Enrique Guitián[1], Gerhard Meyer[2], Leo Gross[2]

[1]Centro de Investigación en Química Biolóxica e Materiais Moleculares (CIQUS) and Departamento de Química Organica, Universidade de Santiago de Compostela Santiago de Compostela, 15782 Spain

[2]IBM Research – Zurich, 8803 Rüschlikon, Switzerland

[3]Molecular Foundry, Lawrence Berkeley National Laboratory, California, USA

4ABB Corporate Research, Baden-Dättwil, Switzerland

Addressing Long-Standing Chemical Challenges by AFM with Functionalized Tips

Diego Peña[1], Niko Pavliček[2], Bruno Schuler[2,3], Nikolaj Moll[2], Dolores Pérez[1], Enrique Guitián[1], Gerhard Meyer[2], Leo Gross[2]

1. Centro Singular de Investigación en Química Biolóxica e Materiais Moleculares (CiQUS) and Departamento de Química Orgánica, Universidade de Santiago de Compostela, 15782 Santiago de Compostela, Spain.
2. IBM Research–Zurich, 8803 Rüschlikon, Switzerland
3. Current affiliation: Molecular Foundry, Lawrence Berkeley National Laboratory, California 94720, USA

Abstract

In this chapter, we illustrate the great potential of combining organic synthesis with atomic resolution AFM and STM to address relevant and classic issues in chemistry, by summarizing selected examples in which we were involved in recent years. As case studies, the long-standing chemical challenges covered here include the experimental discrimination of bond orders in single molecules, the characterization of extremely insoluble compounds such as nanographenes, the analysis of the individual components of complex mixtures, and the on-surface generation and identification of highly reactive molecules and intermediates.

1 Introduction

Undoubtedly, scanning probe microscopy (SPM) is one of the most relevant tools to study surfaces at the nanoscale. First, the introduction of scanning tunneling microscopy (STM) [1], followed by the discovery of atomic force microscopy (AFM) [2], have contributed extensively to the development of diverse scientific fields. In the last decade, SPM has demonstrated to be the crucial technique in the emerging field of on-surface synthesis, to identify and to characterize products resulting from the thermally-induced polymerization of selected monomers on different surfaces [3-8]. On-surface synthesis is an ideal arena for fruitful scientific collaborations between organic chemists and surface physicists who are specialists in SPM: the former design and synthesize suitable molecules in solution while the latter use these molecules as building blocks for on-surface polymerizations (Figure 1). In a seminal experiment [9], 10,10'-dibromo-9,9'-bianthracene was heated on a Au(111) surface to obtain an armchair graphene nanoribbon (7-AGNR) by a sequence of Ullmann couplings followed by cyclodehydrogenation reactions (Figure 2). Since then, new dibromo-substituted polycyclic aromatic compounds have been designed and provided as "à la carte" building blocks to produce GNRs with well-defined widths, edges, and substitution to control the properties and functionality of the final nanostructure. This successful

approach is extensively discussed in other chapters of this volume, as well as in some recent reviews [10-11].
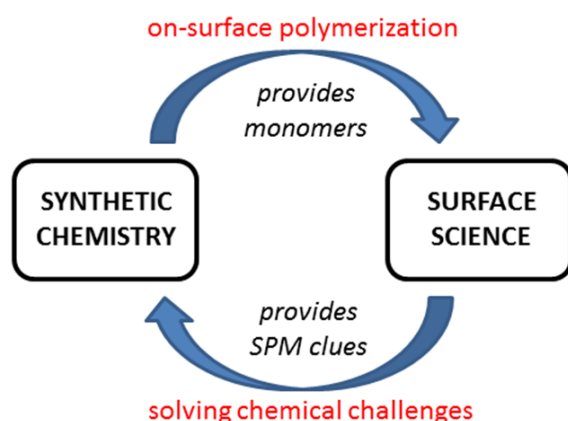

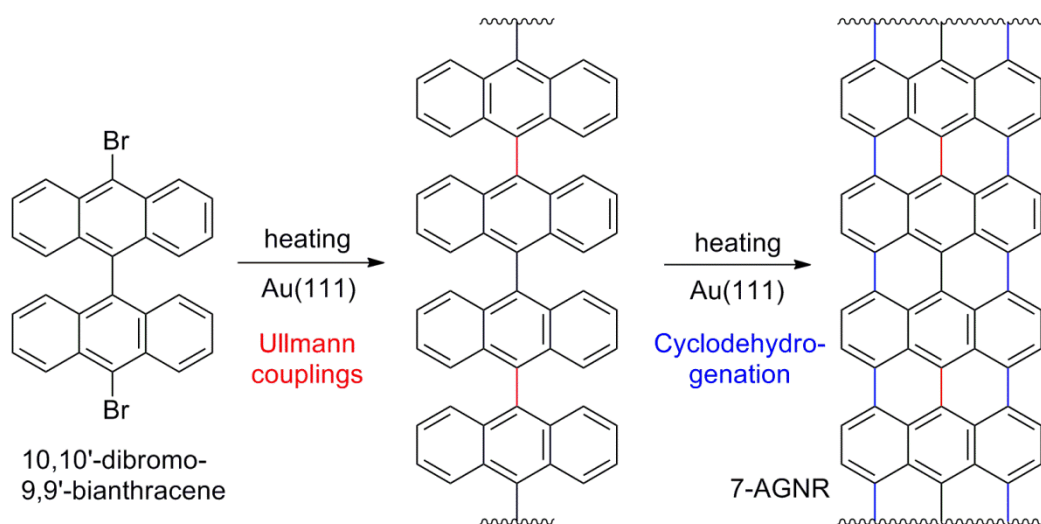Figure 1. Interrelation between synthetic chemistry and surface science.

Figure 2. On-surface preparation of 7-AGNR [9].

Another interesting perspective in this collaborative scenario, which is frequently performed in parallel to the previously mentioned approach, is the topic of this chapter: to take advantage of the clues captured by SPM to answer long-standing chemical questions which are difficult to address with more conventional techniques. In this respect, it has been crucial to achieve sub-molecular resolution in SPM of compounds studied on-surface, a recent breakthrough enabled by the introduction of functionalized tips in AFM under ultrahigh vacuum (UHV) conditions at cryogenic temperatures (5 K) [12]. This finding has provided a privileged methodology to image single molecules with unprecedented resolution and has stimulated a plethora of exciting results in the following years, including the characterization of natural products [13,14], the conformational analysis of diverse molecules [15-17], the identification of intermediates and products of on-surface reactions [18-26], the study of GNR derivatives [27-31] and the characterization of metal-organic complexes on-surface [32-33], among other examples [34-35].

2

In this chapter we discuss the powerful combination of organic synthesis and atomic resolution AFM to address relevant issues in chemistry, by summarizing selected projects in which the authors, chemists from CIQUS and physicists from IBM Research–Zurich, have been involved in recent years.

2 Experimental details

The contrast above bonds and atoms in AFM images of molecules arises from repulsive force contributions due to Pauli repulsion [12,36]. To reach this regime, in which the electron distributions of the molecule and the tip apex start to overlap, the tip is scanned parallel to the surface at a vertical distance of about 4 Å to the molecule. Metallic tip apices are too reactive to reach such small tip-molecule separations. Therefore, it is crucial to terminate (functionalize) the tip apex with an inert front atom or molecule [12]. Most frequently, CO is used, but a wide variety of different terminations has been explored, ranging from single atoms like Cl [12], Br [37], Xe, [37], or O [38] to larger naphthalenetetracarboxylic diimide (NTCDI) molecules [39]. CO-tips are most popular because of their stability, ease of preparation, the localized probing electron density that protrudes from the oxygen atom and the flexibility of the CO at the tip.

Other prerequisites are small oscillation amplitudes of a few tens of picometers to increase the sensitivity to the short-range contributions responsible for the contrast on bonds and atoms [40]. To this end, piezoelectric quartz sensors are operated in frequency-modulation mode [41]. That is, the sensor oscillates with a fixed amplitude at its resonance frequency. The measurement signal is the shift in that resonance frequency, Δf, due to the tip-sample interaction. In the limit of small oscillation amplitudes, Δf is proportional to the vertical gradient of the interaction force. When the frequency shift is recorded as a function of distance, the force can then be calculated numerically [42].

While all experiments presented in this chapter were carried out at temperatures of about T = 5 K using qPlus sensors oscillating at about 30 kHz [43], other works use length extension sensors oscillating at 1 MHz [44, 45]. However, resolution on molecules has also been demonstrated at higher temperatures, at 77 K [39], and even at room temperature using a Si cantilever [46].

3 Pauling bond-order analysis

In 1935, Linus Pauling introduced the concept of bond order to explain the double-bond character found in molecules with single-double bond resonances [47]. Since then, the bond-order analysis has been widely used in chemistry to predict bond lengths and reactivity in a simple manner by drawing the different resonance structures of a molecule. For example, naphthalene has 11 C-C bonds, which can be classified in four kinds of bonds (Figure 3) and three different resonance structures (**1a**, **1b**, **1c**). Focusing on the C1-C2 bond (in red, which is equivalent to C3-C4, C5-C6 or C7-C8), this bond can be drawn as a double bond in structures **1a** and **1b**, but as a single bond in structure **1c**, leading to a 2/3 of double-bond character by the Pauling bond-order analysis. By contrast, the C2-C3 bond (in green, equivalent to C6-C7) can only be drawn as a double bond in the structure **1c**, that means 1/3 of double-bond character. Since greater double-

bond character implies shorter C-C bond distance, this simple analysis suggests C1-C2 to be shorter than C2-C3. This prediction was experimentally proved by X-ray diffraction analysis, which shows that the C1-C2 is shorter than C2-C3 (1.36 Å vs 1.40 Å) [48]. However, diffraction techniques are based on averaged values over a large set of molecules. A tool to analyze bonds within individual molecules with the necessary precision was lacking.
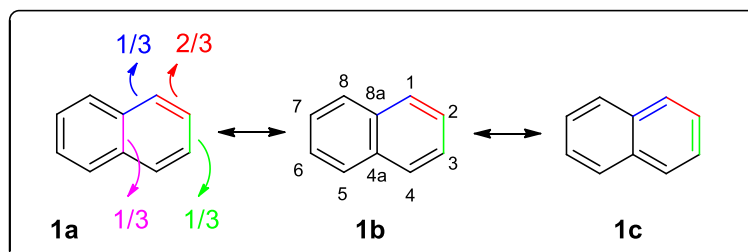

Figure 3. Double-bond character in the four kinds of C-C bonds of naphthalene. The three main resonance structures for naphthalene are **1a**, **1b** and **1c**.

In 2012, it was shown that AFM with CO-terminated tips can discriminate bond orders of organic compounds with high precision [49], based on two effects: the frequency shift of the bonds and the apparent length in constant-height AFM images. The first one is directly related to the different electron densities: the electron density increases with the bond order and greater electron densities give rise to greater repulsive force contributions, which lead to increased frequency shifts. The second effect is related to the tilting of the CO tip which magnifies the apparent bond length differences and provides an additional mechanism to discriminate bond orders. This analysis can be difficult at the edge of the molecules or with non-planar adsorption geometries. On the contrary, bond-order discrimination by AFM is particularly accurate in internal C-C bonds of flat molecules. For example, Figure 4 shows this analysis for dibenzo[*cd,n*]naphtho[3,2,1,8-*pqra*]perylene (DBNP, Fig. 4A), a polycyclic aromatic hydrocarbon (PAH) which was prepared in solution by a sequence of domino Diels-Alder cycloadditions, followed by a reduction and a cyclodehydrogenation reaction [50]. Interestingly, DBNP has five different C-C bonds in the central part of the molecule (*q*, *r*, *s*, *t* and *u*) with calculated bond orders varying from 0.163 (bond *t*) to 0.490 (bond *r*). Indeed, AFM analysis confirmed that bond *r* has the greatest bond order out of these five bonds, by showing the largest frequency shift (Fig. 4B and 4D) and the smallest apparent length (Fig. 4C and 4E) [49]. As we will discuss later, bond-order analysis was found to be particularly useful in the characterization of organic intermediates such as *ortho*-arynes [51] as well as the study of oligoacetylene chains [19].
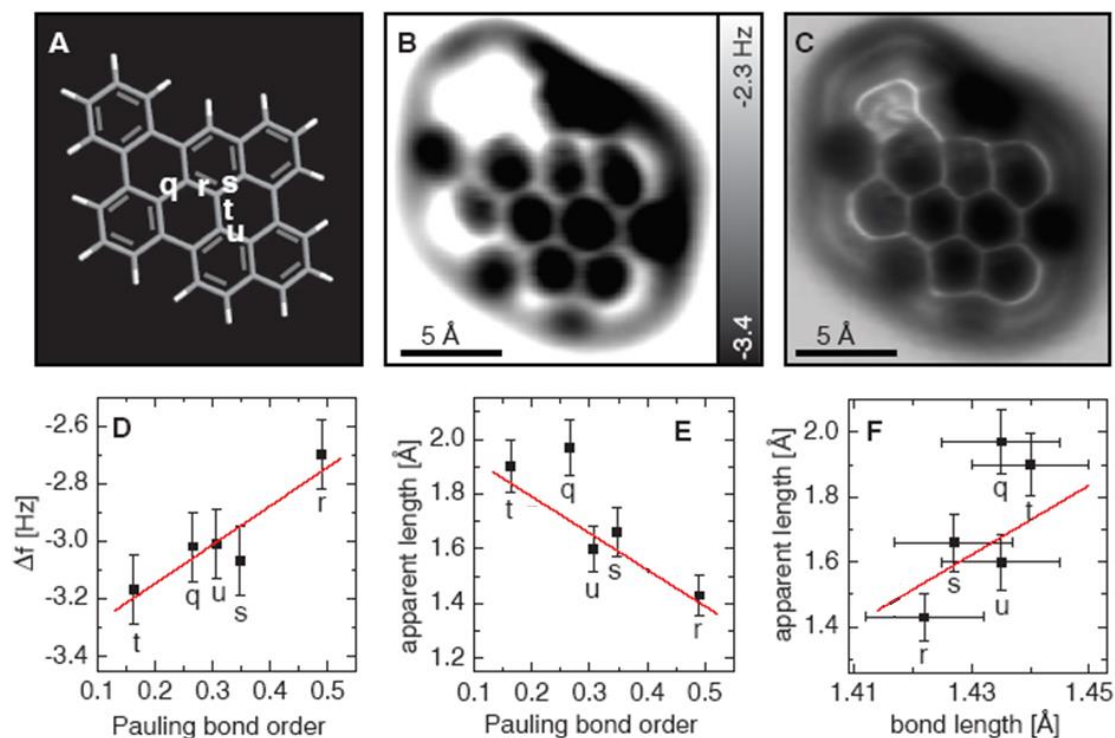
Figure 4. Bond-order analysis for dibenzo[*cd,n*]naphtho[3,2,1,8-*pqra*]perylene (DBNP). A) Structure of DBNP. B) Constant height AFM measurements on bilayer NaCl on Cu(111) at z = 3.6 Å (oscillation amplitude = 0.5 Å). C) Pseudo-3D representation of (B). D) Measured values of the frequency shift as a function of the Pauling bond order. E) Measured values of the apparent bond length as a function of the Pauling bond order. F) Apparent bond length as a function of the bond length obtained by DFT calculations. Linear regressions (in red) are drawn as a guide to the eye. Adapted from [49]. Reprinted with permission from AAAS.

4 Characterization of insoluble compounds: nanographenes

Organic chemists have a deep experience in the manipulation and identification of soluble molecules. Even most nano-sized compounds can be fully characterized by modern spectroscopic techniques, in particular by NMR, if the molecules are soluble enough [52]. On the contrary, the characterization of insoluble compounds is a great challenge for researchers working in an organic chemistry laboratory. This is often the case when preparing large unsubstituted polycyclic aromatic hydrocarbons (PAHs). Interestingly, these molecules are not only ubiquitous environmental pollutants [53, 54] and the largest molecules ever detected in space [55], but PAHs are also promising compounds for organic electronics which have attracted a great deal of attention in material science [56]. Moreover, since a piece of graphene is nothing but a large PAH, the synthesis of large PAHs has undergone an important revival in recent years [57-61]. Synthetic methodologies that were traditionally used for decades for the preparation of PAHs are now employed in the preparation of well-defined nanographenes by solution chemistry. A major limitation is that increasing the size of a PAH favors its self-assembly by means of π-interaction and thereby reducing the solubility of the material. Therefore, the purification of flat

nanographenes by chromatography or its characterization by NMR in solution is not possible. This was the case when we attempted the preparation of the three-fold symmetric nanographene **2** by solution chemistry (Figure 5) [62]. This is a PAH formed by the fusion of 22 benzene rings with 78 sp^2 carbon atoms. We designed an extremely simple two-steps / one-pot procedure starting with commercially available bistriflate **3**. The treatment of this compound with CsF in solution generated the intermediate aryne **4**. This aryne reacted with one of the bay regions of perylene (**5**) by means of a [4+2] cycloaddition (Diels-Alder reaction) to afford adduct **6**, which evolved in the reaction mixture to form triflate **7**. In a second step, which was performed in the same reaction flask, the treatment of compound **7** in solution with CsF in the presence of a catalytic amount of a palladium complex led to the formation of a highly insoluble grayish solid. Based on our experience on aryne chemistry [61], we expected this solid to be nanographene **2**, resulting from the Pd-catalyzed [2+2+2] cycloaddition of the *in-situ* formed aryne **8**. In fact, the mass spectrum of the solid showed a molecular ion at *m/z* = 972.2 consistent with the molecular formula expected for this compound ($C_{78}H_{36}$). However, the extreme insolubility of this compound precluded structural confirmation by NMR spectroscopy.

Inspired by the successful use of AFM for the identification of natural products [13], we attempted to confirm the structure of nanographene **2** analogously. Compound **2** was expected to be planar, an important advantage for the accurate characterization by atomic resolution AFM. However, since purification by chromatography was not possible, the solid isolated from the reaction was far from being a pure compound. In addition, the large size of the molecule could complicate its sublimation to deposit on surface. Despite these limitations, the solid was sublimated by rapid heating from a Si wafer onto a Cu(111) sample partially covered with islands of NaCl held at $T =$ 10 K. Satisfactorily, the analysis by AFM with CO-functionalized tip confirmed the structure of nanographene **2** (Figure 6A). STM was also carried out to obtain molecular orbital images. The image of the negative ion resonance (Figure 6B) corresponds to the lowest unoccupied molecular orbital (LUMO) as seen by comparison with the orbital density squared obtained by DFT calculation (Figure 6C). This agreement is an additional confirmation of the molecular structure, therefore the combination of AFM and STM proved the successful synthesis of compound **2**. Interestingly, careful inspection of other adsorbents by AFM discovered the presence of a tetranaphthoheptacene, an unexpected compound probably formed by the head-to-tail dimerization of aryne **8** [62]. This finding gave additional value to the analysis of reaction mixtures by AFM, where the on-surface identification of byproducts provided key clues to understand the reaction of aryne intermediates in solution.
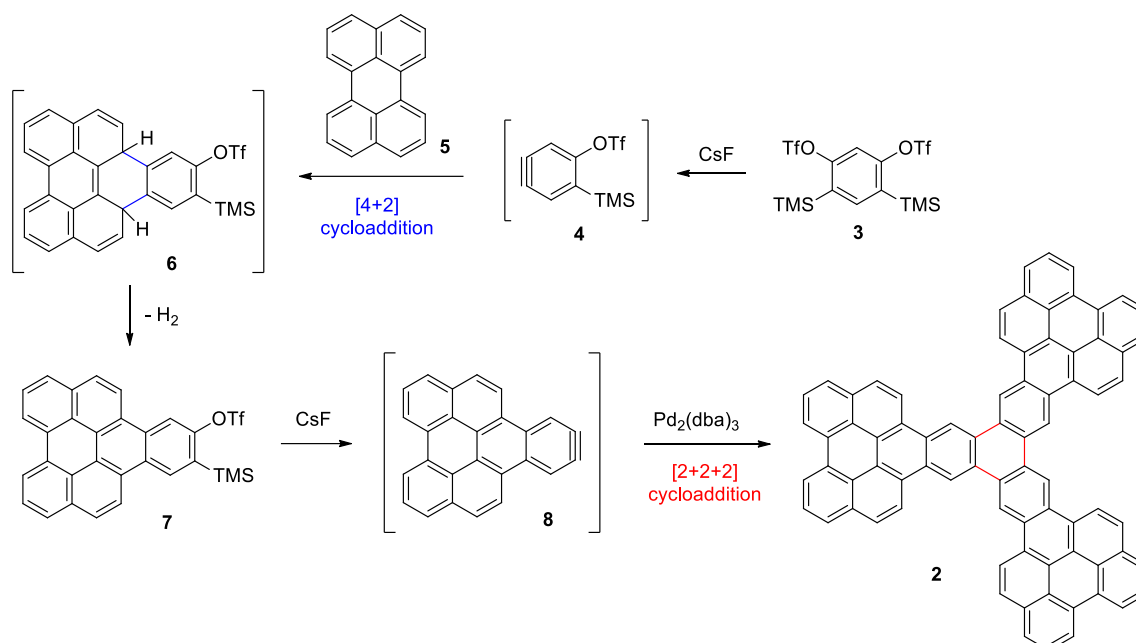
Figure 5. Synthetic route to obtain three-fold symmetric nanographene **2** by solution chemistry [62].
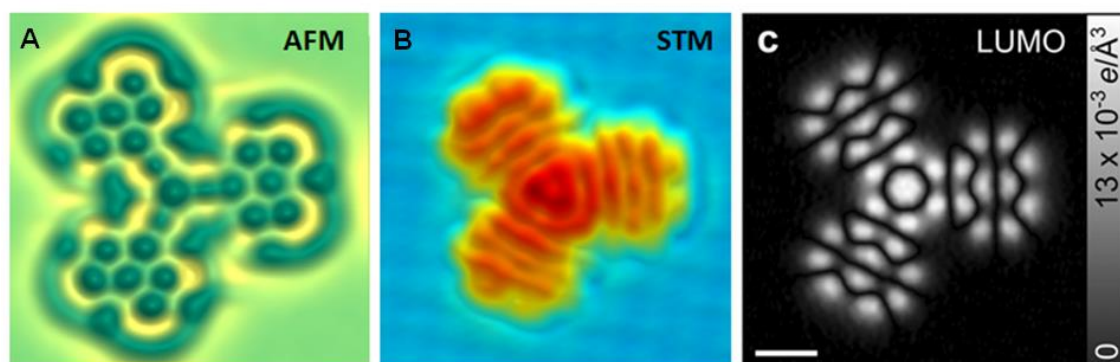

Figure 6. On-surface identification of nanographene **2**. A) AFM image and B) STM orbital image on bilayer NaCl on Cu(111) using a CO tip. C) Calculated orbital density squared of the LUMO at a distance of 1.2 Å above the molecular plane. The scale bar is 5 Å. Adapted from [62]. Copyright Wiley-VCH Verlag GmbH & Co. KGaA. Reproduced with permission.

5 Characterization of complex mixtures: asphaltenes

Usually, SPM studies are performed with ultrapure compounds, since the presence of small amounts of impurities can complicate both the preparation and the study of the sample. However, high resolution SPM can also be extremely useful to analyze complex mixtures by providing the molecular characterization of individual constituents, as it was demonstrated in 2015 by means of asphaltene characterization with atomic resolution AFM [63]. Asphaltenes are the solid components of crude oil, which consist of an extremely complex mixture of polyaromatic molecules with high economic relevance in oil processing [64]. This chemical complexity has limited the structural analysis of asphaltenes by conventional techniques and consequently their molecular architecture has been subject to debates. For example, some studies suggest that the asphaltene molecular structure is based on a single PAH core (*island model*) while other studies point to a structure with multiple PAH cores (*archipelago model*). Notably, the structure elucidation of single molecules of asphaltenes by atomic resolution AFM indicate that the *island*-type architecture is clearly predominant (Figure 7) [63]. As expected, AFM analysis showed the enormous molecular diversity of this fraction. Orbital imaging with STM contributed to the structural assignment of the polyaromatic molecules, which in some cases have sophisticated molecular architectures (e.g. 18-ring nanographene CA6). These findings suggest the exciting possibility of using asphaltenes as an unlimited source of new specimens for single-molecule electronics. Many different molecules can be screened by SPM in a single preparation without going through a lengthy chemical synthesis, purification, and characterization for each one of them beforehand.
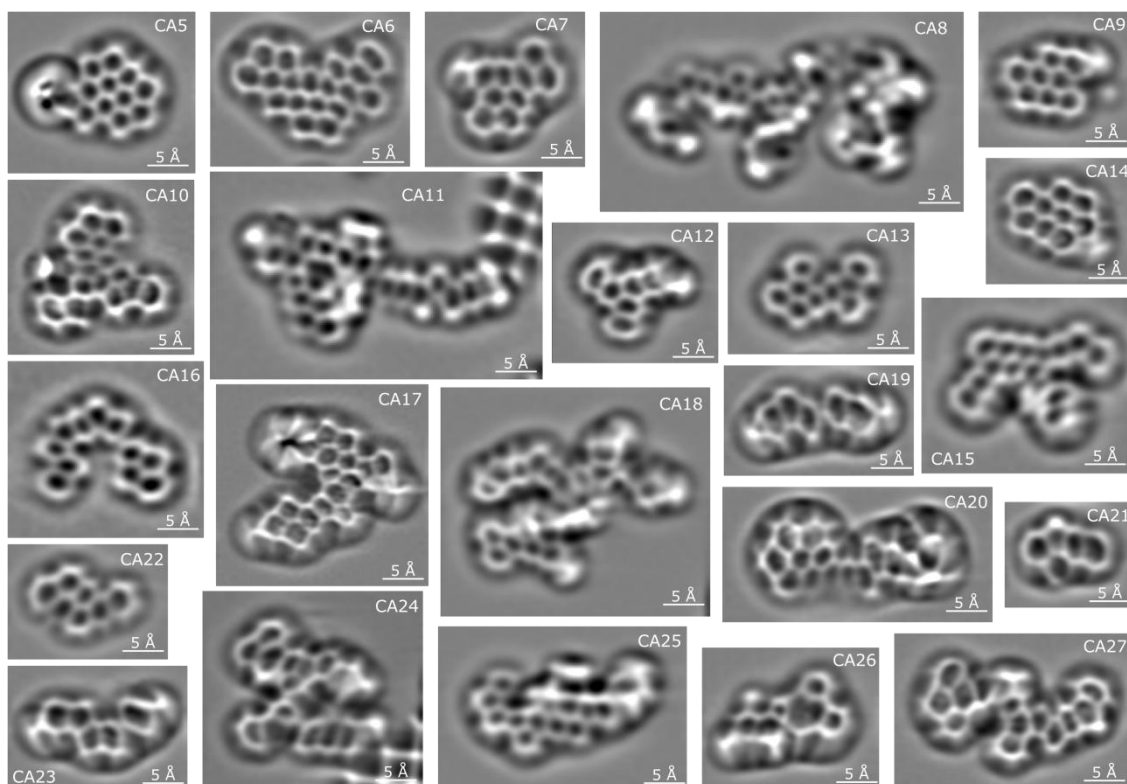
Figure 7. CO-tip AFM images of individual molecules of a coal-derived asphaltene. Reprinted with permission from [63]. Copyright 2015 American Chemical Society.

Obviously, this AFM-based method is not limited to analyze asphaltenes but also related carbon-based aromatic mixtures, such as petroleum and coal vacuum residues, heavy fractions, tar, pitch, bitumen, etc. SPM techniques are most suitable for flat molecules composed mainly by sp^2 hybridized carbons. However, some of the compounds constituting these carbon-based aromatic mixtures present alkyl chains with sp^3 hybridized carbons and non-planar fragments, which are difficult to study by AFM and complicate the structure elucidation. For this reason, the preparation and AFM characterization of model compounds featuring aliphatic moieties can be extremely useful to identify molecules in carbon-based mixtures [17].
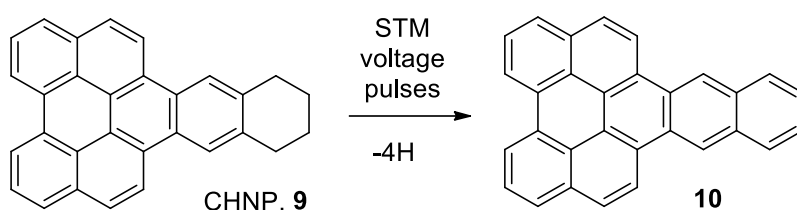

Figure 8. Structure of 10,11,12,13-tetrahydroanthra[1,2,3,4-*ghi*]perylene (CHNP, **9**) used as cycloaliphatic model compound and product **10** resulting from the on-surface STM tip-induced dehydrogenation [17].
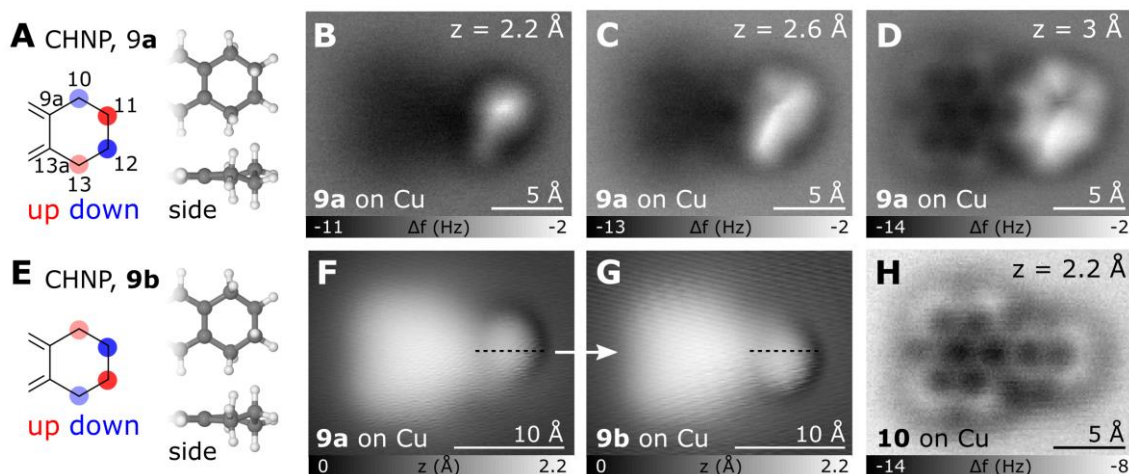
Figure 9. AFM and STM characterization of CHNP, **9**. A, E) Enantiomers **9a** and **9b** of the CHNP structure. B–D) CO tip AFM images of **9a** on Cu(111) at different tip heights. F, G) CO tip STM image of **9a** before (F) and **9b** after (G) enantiomerization by means of a voltage pulse of 0.4 V. H) Molecule **10** after removing four H atoms from the aliphatic ring of **9** with voltage pulses between 3.1 V and 3.8 V. Adapted from [17].

For example, compound **9** (CHNP, Figure 8) was prepared as a cycloaliphatic model compound for asphaltene characterization, with a partially saturated six-membered ring with four sp^3

hybridized carbons. AFM analysis on Cu and NaCl surfaces showed that this cyclohexene moiety adopted the expected chiral half-chair conformation (Figure 9). In fact it was possible to identify both enantiomers (**9a** and **9b**), which were configurationally stable at cryogenic temperatures. Demonstrating the ultimate control of SPM manipulation over on-surface deposited single molecules, reversible enantiomerization (chiral switching) between **9a** and **9b** was induced by applying a STM voltage pulse of 0.4 V (Figure 9F-G). In addition, in a remarkable example of an on-surface oxidation reaction, it was possible to abstract four hydrogen atoms from CHNP by voltage pulses between 3.1-3.8 V, to obtain PAH **10** (Figure 8 and 9H) [17]. To sum up, these experiments illustrate the powerful of on-surface atomic manipulation by SPM, not only to provide key fingerprints of both aromatic and aliphatic moieties for structural elucidation of natural samples, but also to study basic chemical transformations and even to perform conformational analysis of organic molecules on surface.

6 Investigation of elusive molecules: acenes

Acenes are PAHs formed by the linear fusion of several benzene rings, which have been extensively used in organic electronics due to their outstanding semiconducting properties [65]. However, the synthesis and manipulation of acenes under ambient conditions is demanding due to low solubility and high reactivity, in particular with increasing acene length. Qualitative estimation on the stability of PAHs can be deduced by application of the Clar's sextet rule, grouping the π electrons of the PAH into sextets (i.e. three conjugated double bonds within a six-membered ring) [66]. These sextets provide an aromatic stabilization to the molecule, such that PAH with only few Clar sextets are particularly reactive under ambient conditions. Acenes have only one sextet, regardless of the length of the molecule, which explains their instability. Therefore, the synthesis of large acenes has fascinated organic chemists for decades and remains a long-standing synthetic challenge [56]. Up to now, the largest unsubstituted acene ever prepared was nonacene, which was photogenerated and detected in an Ar matrix at cryogenic temperatures [67]. On-surface generation of large acenes under UHV conditions from soluble and stable precursors offers the possibility to circumvent the major difficulties of solution-based acene preparation. This concept has been recently demonstrated with the on-surface reduction of diepoxytetracenes **11** to form tetracene (**13**) on Cu(111), through the formation of intermediate **12** (Figure 10) [68]. It was shown that this transformation can be achieved either by thermal activation or by STM tip-induced manipulation, where the Cu-O interaction is crucial to achieve the deoxygenation of the starting epoxyacenes. This method was latter employed for the on-surface generation of larger acenes, such as the preparation of hexacene on Au(111) by deoxygenation of triepoxyhexacenes (Figure 11A) [69]. As a result, it was possible to study the electronic structure of single hexacene molecules with intramolecular resolution.
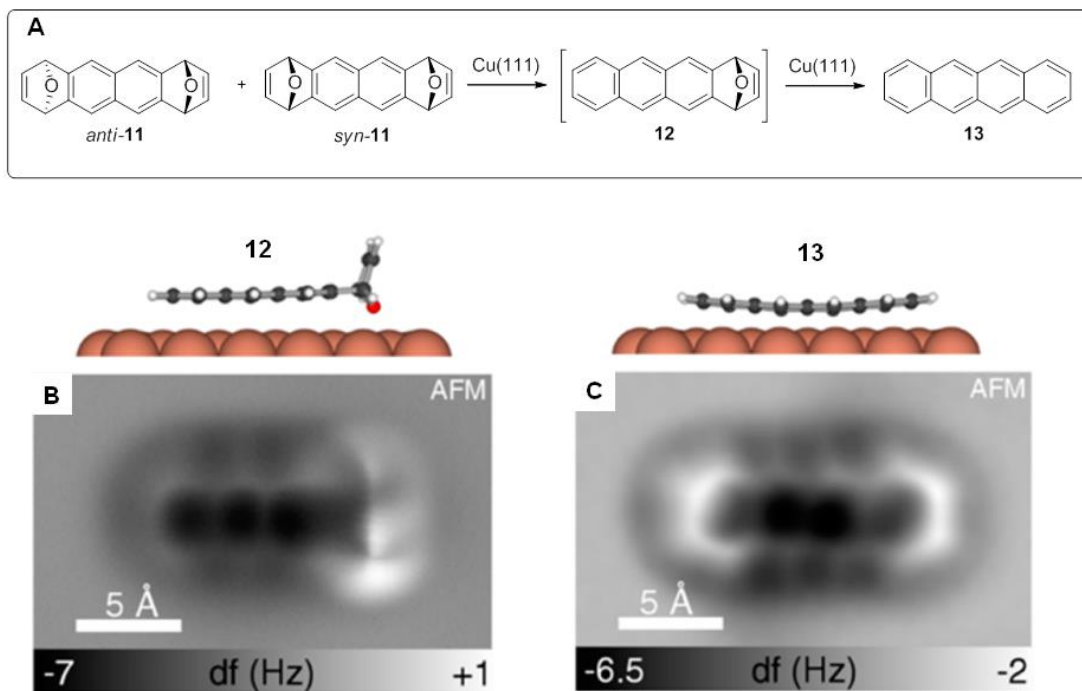
Figure 10. On-surface generation of tetracene (**13**). A) Reaction route to obtain tetracene (**13**) from diepoxytetracenes *syn/anti*-**11**. B) Constant-height AFM image of the epoxytetracene **12** intermediate after the first oxygen detachment. C) Constant-height AFM image of the resulting tetracene (**13**) after complete deoxygenation. Adapted with permission from [68]. Copyright 2016 American Chemical Society.
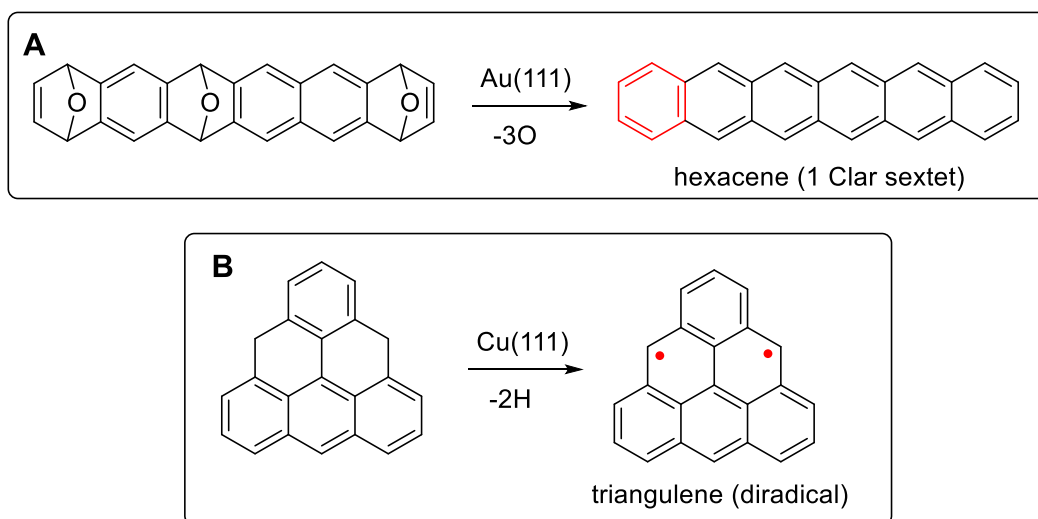

Figure 11. On-surface generation of hexacene (A) [69] and triangulene (B) [70].

A recent breakthrough on the investigation of elusive PAHs was the generation and characterization of triangulene by combined STM/AFM [70]. Triangulene is formed by six benzene

rings fused in a triangle shape, so it is not possible to draw a Kekulé resonance structure and triangulene presents two unpaired electrons (Figure 11B). Therefore, the molecule is a π-diradical which is unstable under ambient conditions, so attempts to generate triangulene by solution chemistry were unsuccessful [71]. Finally, atom manipulation has allowed the preparation of this three-fold symmetric PAH for the first time by means of tip-induced dehydrogenation on Cu, NaCl and Xe surfaces. Notably, STM confirmed the open-shell character of the molecule [70].

7 Investigation of reactive intermediates: arynes

Arynes are reactive intermediates formally derived from arenes by the removal of two hydrogens from one benzene ring [72]. The simplest arynes are benzynes (one single benzene ring), which are classified depending on the relative position of the two unpaired electrons: *ortho* (1,2), *meta* (1,3) or *para* (1,4) (Figure 12). Although arynes were first suggested in 1902 [73], the first evidence of the intermediacy of benzyne in a chemical reaction was established in 1953 by Roberts and coworkers in a seminal isotopic labeling experiment [74]. Arynes are so reactive that they only exist for several milliseconds in solution, making them extremely difficult to characterize. However, structural data of arynes were obtained from UV, IR, microwave and NMR spectroscopies, either in gas phase, using matrix-isolation techniques or in solution after encapsulation inside a hemicarcerand [75], but the interpretation of these data have been the matter of debate. In particular, there is a long-standing discussion about the contribution of diradical **14a**, alkyne **14b** and cumulene **14c** resonance forms to the real structure of *ortho*-arynes (Figure 12A).
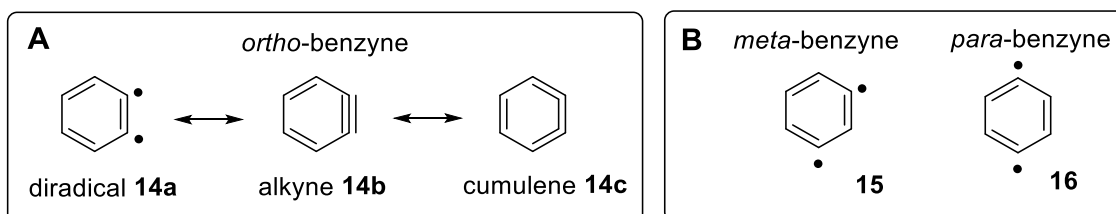

Figure 12. Structure of benzynes, the simplest arynes: *ortho*-benzyne (A), *meta*- and *para*-benzyne (B).

Recently, combined STM/AFM with functionalized tips allowed the on-surface generation and visualization of an aryne (10,11-didehydronaphtho[1,2,3,4-g,h,i]perylene) [51]. The aryne was generated by tip induced cleavage of the two vicinal C-I bonds of 10,11-diiodonaphtho[1,2,3,4-*g,h,i*]perylene (DINP, Figure 13). To this aim, after positioning the tip above DINP, a voltage pulse (V > 1.6 V) was applied. The analysis by atomically resolved AFM using a CO terminated tip, showed the dissociation of both C-I bonds and the formation of the corresponding aryne. To proof that the formed specie retains its arynic nature and reactivity at cryogenic temperature, an additional experiment was performed. After lateral manipulation to place two iodine atoms close to the aryne ring, a voltage pulse was applied causing the reconstruction of the intact DINP

molecule, in contrast to the reactivity of arynes in solution. In addition, the extended planar polyaromatic core facilitated the bond-order analysis of this aryne, following the methodology described in detail in section 2, with the results shown in Figure 14. The bond order evaluation, focused on the central bonds marked on Figure14A, pointed out a dominant contribution of the cumulene resonance structure under these conditions, in good agreement with DFT calculations [51], contributing to clarifying a classic debate in aryne chemistry [72].
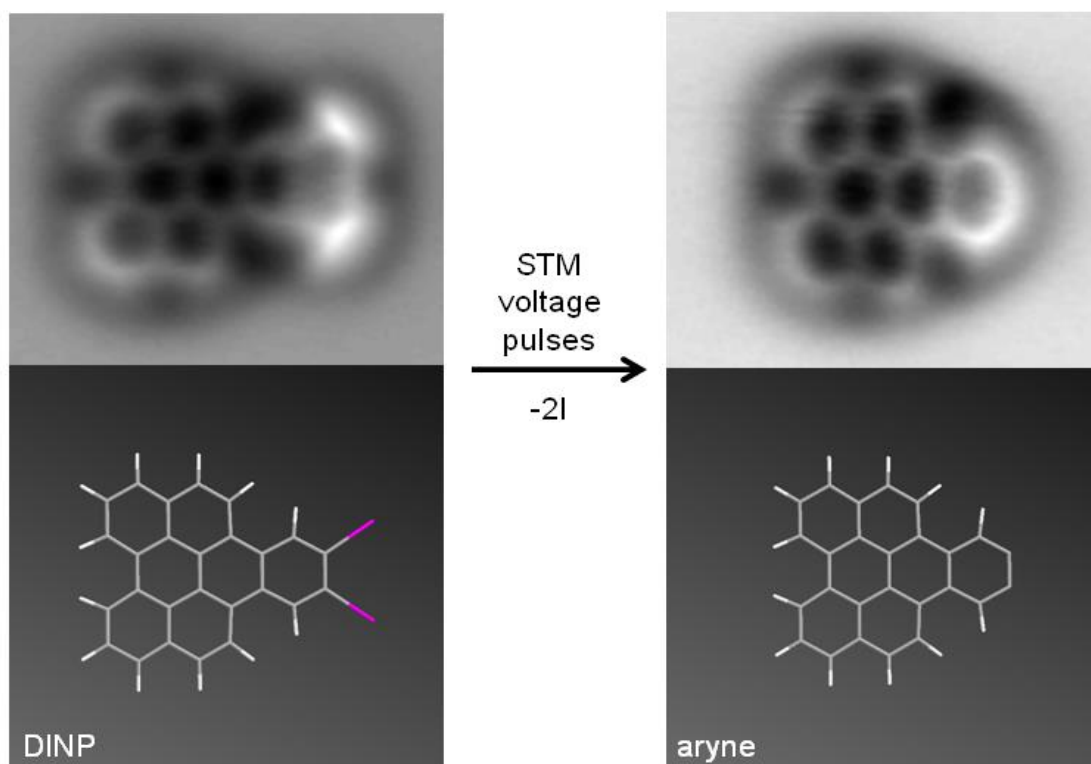

Figure 13. On-surface generation of an *ortho*-aryne (10,11-didehydronaphtho[1,2,3,4-*g,h,i*]perylene) from 10,11-diiodonaphtho[1,2,3,4-*g,h,i*]perylene (DINP). Images with atomic resolution were obtained by non-contact AFM using a CO tip. Adapted from [51] with permission from Nature Publishing Group.
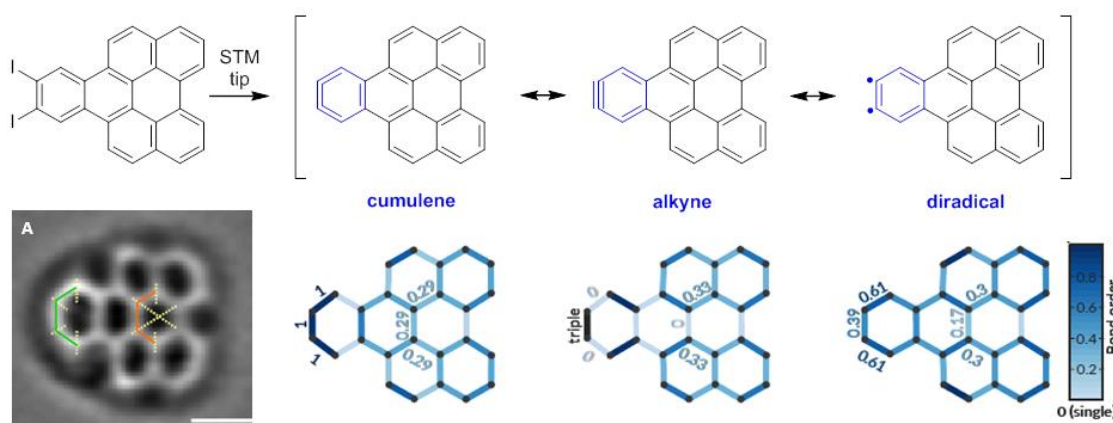
Figure 14. Bond-order analysis of the three major resonance structures of an *ortho*-aryne. A) Laplace-filtered representation of the AFM image of an individual aryne. Adapted from [51] with permission from Nature Publishing Group.

Another type of closely related intermediates are *para*-arynes (Figure 12) [72], sigma-diradical species which can be involved in relevant rearrangement reactions such as the Bergman cyclization. This reaction was first proposed in 1972 to explain the thermal isomerization of enediynes [76], and it became an important transformation in synthetic chemistry when enediyne anticancer antibiotics were introduced in the 80s [77]. Recently, a reversible Bergman cyclization on NaCl was induced by atomic manipulation and studied by combined AFM/STM [78]. Starting with dibromoanthracene (DBA) a sequence of STM voltage pulses induced the cleavage of the two C-Br bonds to generate a *para*-diradical, which evolved to a strained 10-membered ring diyne by means of a retro-Bergman reaction (Figure 15). Notably, the strained diyne could be transformed back into the diradical, demonstrating switching on demand between two intermediates with different reactivity, electronic and magnetic properties.
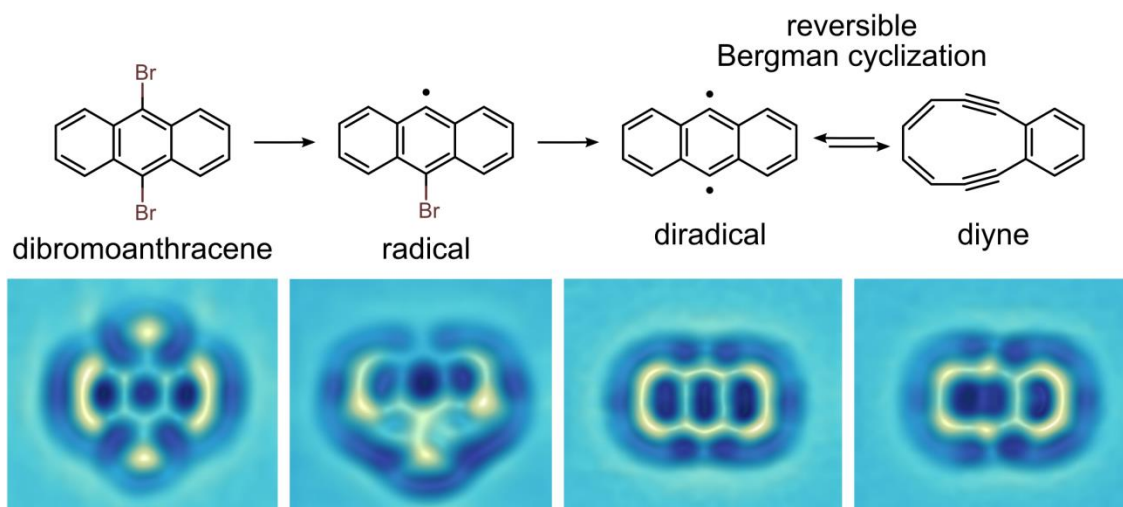

Figure 15. Reversible Bergman cyclization. STM voltage pulses induce the sequential dissociation of two bromine atoms from dibromoanthracene (DBA) to generate a *para*-diradical,

which evolved to a diyne by a retro-Bergman cyclization. The latter transformation can be reversibly triggered by tunneling electrons with a minimum energy of 1.6 V. All measurements were performed on bilayer NaCl on Cu(111). Adapted from [78] with permission from Nature Publishing Group.

8 Conclusions

Atomic resolution AFM and STM by means of functionalized tips is in its infancy, but has already demonstrated an impressive potential regarding to the visualization and manipulation of single atoms and molecules. We are convinced that classic issues in organic chemistry will be revisited using the combination of AFM/STM, mostly to confirm the thesis of chemistry pioneers such as Pauling [36], Clar [55,61], or Roberts [64] as shown in this chapter, but also to discover new molecules, intriguing molecular behavior or unexpected reactions. In fact, the combination of organic chemistry and AFM/STM with sub-molecular resolution is an ideal serendipity playground which is expected to provide exiting findings in the near future. More than ever, we are closer to the inspiring prediction by Richard P. Feynman, masterfully outlined in his famous talk *Plenty of Room at the Bottom* in 1959:

"…it would be, in principle, possible (I think) for a physicist to synthesize any chemical substance that the chemist writes down. Give the orders and the physicist synthesizes it. How? Put the atoms down where the chemist says, and so you make the substance. The problems of chemistry and biology can be greatly helped if our ability to see what we are doing, and to do things on an atomic level, is ultimately developed— a development which I think cannot be avoided."

References

[1] Binnig, G., Rohrer, H., Gerber, C., Weibel, E.: Tunneling through a controllable vacuum gap. Appl. Phys. Lett. **40**, 178–180 (1982).

[2] Binnig, G., Quate, C.F., Gerber, C.: Atomic force microscope. Phys. Rev. Lett. **56**, 930–933 (1986).

[3] Grill, L., Dyer, M., Lafferentz, L., Persson, M., Peters, M.V., Hecht, S.: Nano-architectures by covalent assembly of molecular building blocks. Nat. Nanotechnol. **2**, 687–691 (2007).

[4] Franc, G., Gourdon, A.: Covalent networks through on-surface chemistry in ultra-high vacuum: state-of-the-art and recent developments. Phys. Chem. Chem. Phys. **13**, 14283−14292 (2011).

[5] Klappenberger, F., Zhang, Y.-Q., Björk, J., Klyatskaya, S., Ruben, M., Barth, J.V.: On-Surface Synthesis of Carbon-Based Scaffolds and Nanomaterials Using Terminal Alkynes. Acc. Chem. Res. **48**, 2140–2150 (2015).

[6] Lindner, R., Kühnle, A.: On-surface reactions. Chem. Phys. Chem. **16**, 1582–1592 (2015).

[7] Méndez, J., Francisca López, M., Martín-Gago, J.A.: On-surface synthesis of cyclic organic molecules. Chem. Soc. Rev. **40**, 4578–4590 (2011).

[8] Nacci, C., Hecht, S., Grill, L.: The Emergence of Covalent On-Surface Polymerization in *On-Surface Synthesis*, Springer, S. 1–21 (2016).

[9] Cai, J., Ruffieux, P., Jaafar, R., Bieri, M., Braun, T., Blankenburg, S., Muoth, M., Seitsonen, A.P., Saleh, M., Feng, X., Müllen, K., Fasel, R.: Atomically precise bottom-up fabrication of graphene nanoribbons. Nature **466**, 470–473 (2010).

[10] Narita, A., Feng, X., Müllen, K.: Bottom-Up Synthesis of Chemically Precise Graphene Nanoribbons. Chem. Rec. **15**, 295-309 (2015).

[11] Talirz, L., Ruffieux, P., Fasel, R.: On-Surface Synthesis of Atomically Precise Graphene Nanoribbons. Adv. Mater. **28**, 6222–6231 (2016).

[12] Gross, L., Mohn, F., Moll, N., Liljeroth, P., Meyer, G.: The chemical structure of a molecule resolved by atomic force microscopy. Science **325**, 1110-1114 (2009).

[13] Gross, L., Mohn, F., Moll, N., Meyer, Ebel, G.R., Abdel-Mageed, W.M., Jaspars, M.: Organic structure determination using atomic resolution scanning probe microscopy. Nat. Chem. **2**, 821-825 (2010).

[14] Hanssen, K.O., Schuler, B., Williams, A., Demissie, T.B., Hansen, E., Andersen, J.H., Svenson, J., Blinov, K., Repisky, M., Mohn, F., Meyer, G., Svendsen, J.-S., Ruud, R., Elyashberg, M., Gross, L., Jaspars, M., Isaksson, J.: A combined atomic force microscopy and computational approach for structural elucidation of breitfussin A and B, highly modified halogenated dipeptides from the Arctic hydrozoan *Thuiaria breitfussi*. Angew. Chem. Int. Ed. **51**, 12238–12241 (2012).

[15] Pavliček, N., Fleury, B., Neu, M., Niedenführ, J., Herranz-Lancho, C., Ruben, M., Repp, J.: Atomic force microscopy reveals bistable configurations of dibenzo[a,h]thianthrene and their interconversion pathway. Phys. Rev. Lett. **108**, 086101 (2012).

[16] Albrecht, F., Bischoff, F., Auwärter, W., Barth, J.V., Repp, J.: Direct Identification and Determination of Conformational Response in Adsorbed Individual Nonplanar Molecular Species Using Noncontact Atomic Force Microscopy. Nano Lett. **16**, 7703–7709 (2016).

[17] Schuler, B., Zhang, Y., Collazos, S., Fatayer, S., Meyer, G., Pérez, D., Guitián, E., Harper, M.R., Kushnerick, J.D., Peña, D., Gross, L.: Characterizing aliphatic moieties in hydrocarbons with atomic force microscopy. Chem. Sci. **8**, 2315–2320 (2017).

[18] de Oteyza, D.G., Gorman, P., Chen, Y.-C., Wickenburg, S., Riss, A., Mowbray, D.J., Etkin, G., Pedramrazi, Z., Tsai, H.-Z., Rubio, A., Crommie, M.F., Fischer, F.R.: Direct imaging of covalent bond structure in single-molecule chemical reactions. Science **340**, 1434–1437 (2013).

[19] Riss, A., Wickenburg, S., Gorman, P., Tan, L.Z., Tsai, H.-Z., de Oteyza, D.G., Chen, Y.-C., Bradley, A.J., Ugeda, M.M., Etkin, G., Louie, S.G., Fischer, F.R., Crommie, M.F.: Local Electronic and Chemical Structure of Oligo-acetylene Derivatives Formed Through Radical Cyclizations at a Surface. Nano Lett. **14**, 2251–2255 (2014).

[20] Rogers,C., Chen, C., Pedramrazi, Z., Omrani, A.A., Tsai, H.-Z., Jung, H.S., Lin, S., Crommie, M.F., Fischer, F.R.: Closing the nanographene gap: surface-assisted synthesis of peripentacene from 6,6´-bipentacene precursors. Angew. Chem. Int. Ed. **54**, 15143–15146 (2015).

[21] Albrecht, F., Pavliček, N., Herranz-Lancho, C., Ruben, M., Repp, J.: Characterization of a surface reaction by means of atomic force microscopy. J. Am. Chem. Soc. **137**, 7424–7428 (2015).

[22] Kawai, S., Haapasilta, V., Lindner, B.D., Tahara, K., Spijker, P., Buitendijk, J.A., Pawlak, R., Meier, T., Tobe, Y., Foster, A.S., Meyer, E.: Thermal control of sequential on-surface transformation of a hydrocarbon molecule on a copper surface. Nat. Comm. **7**, 12711 (2016).

[23] He, Y., Garnica,M., Bischoff, F., Ducke, J., Bocquet, M.-L., Batzill, M., Auwärter, W., Barth, J.V.: Fusing tetrapyrroles to graphene edges by surface-assisted covalent coupling. Nat. Chem. **9**, 33–38 (2017).

[24] Kocic, N., Liu, X., Chen, S., Decurtins, S., Krejcí, O., Jelínek,P., Repp, J., Liu, S.-X.: Control of Reactivity and Regioselectivity for On-Surface Dehydrogenative Aryl–Aryl Bond Formation. J. Am. Chem. Soc. **138**, 5585–5593 (2016).

[25] Riss, A., Paz, A.P., Wickenburg, S., Tsai, H.-Z., de Oteyza, D.G., Bradley, A.J., Ugeda, M.M., Gorman, P., Jung, H.S., Crommie, M.F., Rubio, A., Fischer, F.R.: Imaging single-molecule reaction intermediates stabilized by surface dissipation and entropy. Nat. Chem. **8**, 678–683 (2016).

[26] Stetsovych, O., Švec, M., Vacek, J., Chocholoušová, J.V., Jancark, A., Rybácek, J., Kosmider, K., Stará, I.G., Jelnek, P., Stary, I.: From helical to planar chirality by on-surface chemistry. Nat. Chem. **9**, 213–218 (2017).

[27] van der Lit, J., Boneschanscher, M.P., Vanmaekelbergh, D., Ijäs, M., Uppstu, A., Ervasti, M., Harju, A., Liljeroth, P., Swart, I.: Suppression of electron–vibron coupling in graphene nanoribbons contacted via a single atom. Nat. Comm. **4**, 2023 (2013).

[28] Ruffieux, P., Wang, S., Yang, B., Sánchez-Sánchez,C., Liu, J., Dienel, T., Talirz, L., Shinde, P., Pignedoli, C.A., Passerone, D., Dumslaff, T., Feng, X., Müllen, K., Fasel, R.: On-surface synthesis of graphene nanoribbons with zigzag edge topology. Nature **531**, 489–492 (2016).

[29] Schulz, F., Jacobse, P.H., Canova, F.F., van der Lit, J., Gao, D.Z., van den Hoogenband, A., Han, P., Klein Gebbink, R.J.M., Moret, M.-E., Joensuu, P.M., Swart, I., Liljeroth, P.: Precursor Geometry Determines the Growth Mechanism in Graphene Nanoribbons. J. Phys. Chem. C **121**, 2896–2904 (2017).

[30] Kawai, S., Saito, S., Osumi, S., Yamaguchi, S., Foster, A.S., Spijker, P., Meyer, E.: Atomically controlled substitutional boron-doping of graphene nanoribbons. Nat. Comm. **6**, 8098 (2015).

[31] Dienel, T., Kawai, S., Söde, H., Feng, X., Müllen, K., Ruffieux, P., Fasel, R., Gröning, O.: Resolving atomic connectivity in graphene nanostructure junctions. Nano Lett. **15**, 5185–5190 (2015).

[32] Mohn, F., Repp, J., Gross, L., Meyer, G., Dyer, M. S., Persson, M.: Reversible bond formation in a gold-atom–organic-molecule complex as a molecular switch. Phys. Rev. Lett. **105**, 266102 (2010).

[33] Albrecht, F., Neu, M., Quest, C., Swart, I., Repp, J.: Formation and characterization of a molecule–metal– molecule bridge in real space. J. Am. Chem. Soc. **135**, 9200–9203 (2013).

[34] Gross, L., Schuler, B., Mohn, F., Moll, N., Repp, J., Meyer, G.: Atomic Resolution on Molecules with Functionalized Tips in *Noncontact Atomic Force Microscopy* (S. Morita, F. J. Giessibl, E. Meyer, R. Wiesendanger), Springer S. 223–246 (2015).

[35] Pavliček, N., Gross, L.: Generation, manipulation and characterization of molecules by atomic force microscopy. Nat. Rev. Chem. **1**, 0005 (2017).

[36] Moll, N., Gross, L., Mohn, F., Curioni, A., Meyer, G.: A simple model of molecular imaging with noncontact atomic force microscopy. New J. Phys. **14**, 083023 (2012).

[37] Mohn, F., Schuler, B., Gross, L., Meyer, G.: Different tips for high-resolution atomic force microscopy and scanning tunneling microscopy of single molecules. Appl. Phys. Lett. **102**, 073109–5 (2013)

[38] Mönig, H., Hermoso, D.R., Arado, O.D., Todorović, M., Timmer, A., Schüer, S., Langewisch, G., Pérez, R., Fuchs, H.: Submolecular Imaging by Noncontact Atomic Force Microscopy with an Oxygen Atom Rigidly Connected to a Metallic Probe. ACS Nano. **10**, 1201–1209 (2015).

[39] Sweetman, A.M., Jarvis, S.P., Sang, H., Lekkas, I., Rahe, P., Wang, Y., Wang, J., Champness, N.R., Kantorovich, L.N., Moriarty, P.: Mapping the force field of a hydrogen-bonded assembly. Nature Comm. **5**, 3931 (2014).

[40] Giessibl, F. J.: Advances in atomic force microscopy. Rev. Mod. Phys. **75**, 949–983 (2003).

[41] Albrecht, T. R., Grütter, P., Horne, D., Rugar, D.: Frequency modulation detection using high-Q cantilevers for enhanced force microscope sensitivity. J. Appl. Phys. **69**, 668–673 (1991).

[42] Sader, J. E., Jarvis, S. P.: Accurate formulas for interaction force and energy in frequency modulation force spectroscopy. Appl. Phys. Lett. **84**, 1801–1803 (2004).

[43] Giessibl, F.J.: High-speed force sensor for force microscopy and profilometry utilizing a quartz tuning fork. Appl. Phys. Lett. **73**, 3956–4 (1998).

[44] Hapala, P., Švec, M., Stetsovych, O., van der Heijden, N.J., Ondráček, M., van der Lit, J., Mutombo, P., Swart, I., Jelínek, P.: Mapping the electrostatic force field of single molecules from high-resolution scanning probe images. Nature Comm. **7**, 11560 (2016).

[45] Stetsovych, O., Švec, M., Vacek, J., Chocholoušová, J.V., Jančařík, A., Rybáček, J., Kosmider, K., Stará, I.G., Jelínek, P., Starý, I.: From helical to planar chirality by on-surface chemistry. Nature Chem. **9**, 213–218 (2017).

[46] Iwata, K., Yamazaki, S., Mutombo, P., Hapala, P., Ondráček, M., Jelínek, P., Sugimoto, Y.: Chemical structure imaging of a single molecule by atomic force microscopy at room temperature. Nature Comm. **6**, 7766 (2015).

[47] Pauling, L., Brockway, L.O., Beach, J.Y.: The Dependence of Interatomic Distance on Single Bond-Double Bond Resonance. J. Am. Chem. Soc. **57**, 2705-2709 (1935).

[48] Abrahams, S.C., Robertson, J. M., White, J.G.: The Crystal and Molecular Structure of Naphthalene. Acta Cryst. **2**, 238-244 (1949).

[49] Gross, L., Mohn, F., Moll, N., Schuler, B., Criado, A., Guitián, E., Peña, D., Gourdon, A., Meyer, G.: Bond-Order Discrimination by Atomic Force Microscopy. Science **337**, 1326-1329 (2012).

[50] Criado, A., Peña, D., Cobas, A., Guitián, E.: Domino Diels–Alder Cycloadditions of Arynes: New Approach to Elusive Perylene Derivatives. Chem. Eur. J. **16**, 9736-9740 (2010).

[51] Pavliček, N., Schuler, B., Collazos, S., Moll, N., Pérez, D., Guitián, E., Meyer, G., Peña, D., Gross, L.: On-surface generation and imaging of arynes by atomic force microscopy. Nat. Chem. **7**, 623–628 (2015).

[52] Silverstein, R.M., Webster, F.X., Kiemle, D.J. Bryce, D. L.: Spectrometric Identification of Organic Compounds, 8th Edition, Wiley (2014).

[53] Harvey, R. G.: Polycyclic Aromatic Hydrocarbons, Wiley, New York, (1997).

[54] Lunch, A.: The Carcinogenic Effects of Polycyclic Aromatic Hydrocarbons, Imperial College Press, London (2005).

[55] Tielens, A.G.M.: Interstellar Polycyclic Aromatic Hydrocarbon Molecules. Ann. Rev. Astron. Astrophys. **46**, 289–337 (2008).

[56] Anthony, J.E.: The Larger Acenes: Versatile Organic Semiconductors, *Angew. Chem. Int. Ed.* **47**, 452–483 (2008).

[57] Peña, D.: Ideas in Chemistry and Molecular Sciences: Advances in Synthetic Chemistry, Wiley, Weinheim, Germany, p. 237–261 (2010).

[58] Chen, L., Hernandez, Y., Feng, X., Müllen, K: From Nanographene and Graphene Nanoribbons to Graphene Sheets: Chemical Synthesis. Angew. Chem. Int. Ed. **51**, 7640–7654 (2012).

[59] Narita, A., Wang, X.-Y., Feng, X., Müllen, K.: New advances in nanographene chemistry. Chem. Soc. Rev. **44**, 6616-6643 (2015).

[60] Itami, K.: Toward controlled synthesis of carbon nanotubes and graphenes. Pure Appl. Chem. **84**, 907–916 (2012).

[61] Pérez, D., Peña, D., Guitián, E.: Aryne Cycloaddition Reactions in the Synthesis of Large Polycyclic Aromatic Compounds. Eur. J. Org. Chem. 5981–6013 (2013).

[62] Schuler, B., Collazos, S., Gross, L. Meyer, G., Pérez, D., Guitián, E., Peña, D.: From Perylene to a 22-Ring Aromatic Hydrocarbon in One-Pot. Angew. Chem. Int. Ed. **53**, 9004-9006 (2014).

[63] Schuler, B., Meyer, G., Peña, D., Mullins, O.C., Gross, L.: Unraveling the Molecular Structures of Asphaltenes by Atomic Force Microscopy. J. Am. Chem. Soc. **137**, 9870 (2015).

[64] Mullins, O.C., Sheu, E.Y. Hammami, A. Marshall, A.G.: Asphaltenes, Heavy Oils, and Petroleomics, Springer (New York), vol. 1 (2007).

[65] Ye, Q., Chi, C.: Recent Highlights and Perspectives on Acene Based Molecules and Materials. Chem. Mater. **26**, 4046−4056 (2014).

[66] Clar, E.: The Aromatic Sextet, Wiley, New York, (1972).

[67] Tönshoff, C., Bettinger, H.F.: Photogeneration of Octacene and Nonacene. Angew. Chem. Int. Ed. **49**, 4125-4128 (2010).

[68] Krüger, J., Pavliček, N., Alonso, J.M., Pérez, D., Guitián, E., Lehmann, T., Cuniberti, G., Gourdon, A., Meyer, G., Gross, L., Moresco, F., Peña, D.: Tetracene Formation by On-Surface Reduction. ACS Nano **10**, 4538-4542 (2016).

[69] Krüger, J., Eisenhut, F., Alonso, J.M., Lehmann, T., Guitián, E., Pérez, D., Skidin, D., Gamaleia, F., Ryndyk, D.A., Joachim, C., Peña, D., Moresco, F., Cuniberti, G.: Imaging the electronic structure of on-surface generated hexacene. Chem. Commun. **53***, 1583-1586 (2017).

[70] Pavliček, N., Mistry, A., Majzik, Z., Moll, N., Meyer, G., Fox, D.J., Gross, L.: Synthesis and characterization of triangulene. *Nat. Nano.* 12, 308-312 (2017).

[71] Clar, E., Stewart, D.: Aromatic hydrocarbons. LXV. Triangulene derivatives 1. J. Am. Chem. Soc. **75**, 2667–2672(1953).

[72] Wenk, H. H., Winkler, M., Sander, W.: One century of aryne chemistry. Angew. Chem. Int. Ed. 42, 502–528 (2003).

[73] Störmer, R., Kahlert, B.: Über das 1- und 2-Brom-cumaron. *Ber. Dtsch. Chem. Ges.* **35**, 1633-1640 (1902).

[74] Roberts, J.D., Simmons, H.E., Carlsmith, L.A., Vaughan, C.W.: Rearrangement in the reaction of chlorobenzene-1-14C with potassium amide. J. Am. Chem. Soc. **75**, 3290-3291 (1953).

[75] Warmuth, R.: *o*-Benzyne: Strained Alkyne or Cumulene?—NMR Characterization in a Molecular Container. Angew. Chem. Int. Ed. Engl. **36**, 1347-1350 (1997).

[76] Jones, R.R., Bergman, R.G.: p-Benzyne. Generation as an intermediate in a thermal isomerization reaction and trapping evidence for the 1,4-benzenediyl structure. J. Am. Chem. Soc. **94**, 660–661 (1972)

[77] Nicolaou, K.C., Dai, W.-M., Tsay, S.-C., Estevez, V.A., Wrasidlo, W.: Designed enediynes: a new class of DNA-cleaving molecules with potent and selective anticancer activity. Science **256**, 1172–1178 (1992).

[78] Schuler, B., Fatayer, S., Mohn, F., Moll, N., Pavliček, N., Meyer, G., Peña, D., Gross, L.: Reversible Bergman cyclization by atomic manipulation. Nat. Chem. **8**, 220-224 (2016).

Advances in Atom and Single Molecule Machines
Volume: On-Surface Synthesis II
Volume Editors: Dimas G. de Oteyza and Celia Rogero